WELDING RESEARCH

SUPPLEMENT TO THE WELDING JOURNAL, JULY 1975

Sponsored by the American Welding Society and the Welding Research Council

Particulate Fume Generation Arc Welding Processes

Mechanisms of particulate emission along with emission rates and composition have been determined for a variety of arc welding processes

BY R. F. HEILE AND D. C. HILL

ABSTRACT. A technical method has been developed that allows a determination of the fume formation rate and fume composition in arc welding processes. This method has been used to characterize particulate emissions in a number of processes: shielded metal arc (SMA), gas metal arc (GMA), flux cored arc (FCA), and gas tungsten arc (GTA) welding, and has permitted a ranking of these processes according to their relative "cleanliness." Of the continuous electrode processes studied, GMA welding with argon-based shielding gas produced the least fumes, while self-shielding FCA welding produced the most. The data indicate that the mechanism of fume formation is one of elemental vaporization-condensation and oxidation enhanced vaporization-condensation of the consumable constituents. A model relating this mechanism to process and process variables is advanced which would allow fume formation rates and composition to be predicted semi-quantitatively given a knowledge of the consumable composition, the volatility of the constituents, the transfer mode, the arc temperature and stability as determined by the welding parameters and shield gas, and the oxidizing potential of the shield gas. Based on the results, methods of fume control are indicated which can serve as a supplement to ventilation.

R. F. HEILE is Senior Research Physicist and D. C. HILL is Group Leader, Linde Research Department, Linde Division, Union Carbide Corporation, Tarrytown, New York 10591.

Introduction

Although numerous studies of the generation of smoke and fume in arc welding have been made (Ref. 1), the mechanism and character of the fume formation have not been extensively investigated or reported. It is now recognized that variations in sampling techniques, electrode compositions, and welding parameters all have a major impact on the results of fume experiments. As a result, care must be exercised in interpreting the existing literature. Recently, a proposed technique for measurement of fume generation in arc welding has been published (Ref. 2). Unfortunately, little statistical evidence for the accuracy and reproducibility of this technique was advanced.

The purposes of this study are to provide fume generation comparisons among different arc welding processes, to understand the mechanism of fume formation, and to supply the information necessary for choice of a welding process when ventilation considerations are important.

Method for Particulate Sampling

General

A critical aspect of particulate sampling is the technique itself. Various sampling techniques have been employed by other investigators (Ref. 1). Many of these techniques collect all of the evolved fume. In so doing, oftentimes unrealistic conditions are imposed on the particular welding process. We chose, instead, to use a modified stack sampling technique which would minimally disturb the welding process and at the same time allow a carefully controlled sample to be taken at a predetermined rate. This section briefly describes the technique and discusses the accuracy and reproducibility of the results.

Experimental Technique

A schematic of the stack sampling system employed in this work is shown in Fig. 1. A duct was placed coaxially over a stationary welding torch. Welds were made on a rotating workpiece. The gas flow rate of the duct was set to allow collection of most all the fume, yet not so fast as to disturb the shielding gas. The duct velocity was measured using an inclined manometer. A probe, connected to a filter and a sampling pump, was inserted in the duct. The velocity in the probe was adjusted to match the duct velocity. By maintaining isokinetic sampling conditions, it is possible to relate the size of the sample collected to the total fume evolution without having to collect all of the fume.

This technique is applicable over a range of duct velocities, i.e., sampling rates for a constant sampling time. This is especially important in sampling emissions where the saturation time of the filter is short. Without control over the sampling rate in such situations, the results would be subject to transient effects related to short sampling times. This technique eliminates those problems.

The basic procedure followed for taking a sample was to establish isokinetic sampling conditions and then, before actually beginning the sample, to choose the welding parameters. Sampling was begun after the arc was struck and steady-state conditions established. The duration of the sampling period depended upon the fume formation rate and the filter capacity. The importance of the sampling period is discussed in greater detail in the section below.

Two types of filters were employed, glass fiber filters and triacetate filters. The glass fiber filters were used principally to determine the fume generation rates, and the triacetate filters were used to collect fume for chemical analysis. Typical sampling times were 2 minutes for the glass fiber filters and 30 seconds for the triacetate filters.

An optical viewing system attached to the welding station permitted a simple measurement of arc length.

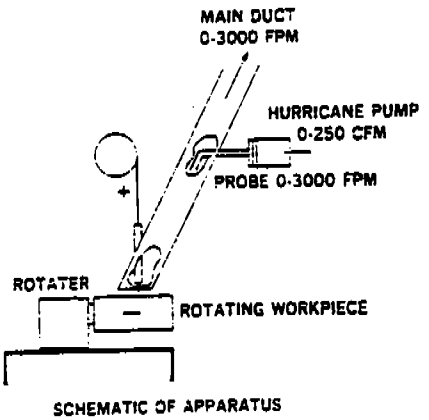

Fig. 1 — Schematic diagram of fume sampling apparatus

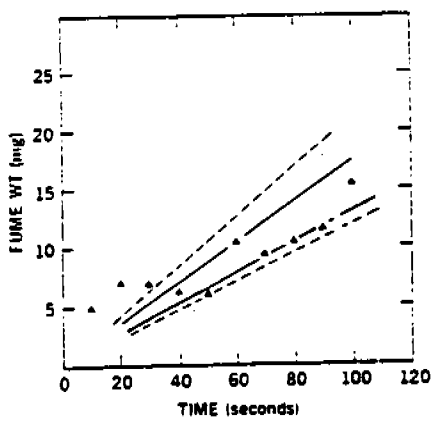

Fig. 2 — Variations and collection efficiencies for several filters as a function of time

Reproducibility and Variations

The purpose of sampling is, of course, to arrive at a fume formation rate (FFR) and a fume composition which can be assigned to a given welding process. It is obvious that the generation rate will depend upon voltage and current as well as the process and that the fume generation rate must be expressed as a function of these or related parameters. It is not so obvious how sensitive fume formation is to such things as work travel speed and variations in the plates on which the welds are made or, for that matter, to the sampling procedure itself.

In order to assess the accuracy of these experiments and to determine what parameters are needed to specify FFRs unambiguously, a two-fold investigation was undertaken. This included an investigation of the dependence of fume formation on voltage, current, work travel speed, and plate variations and an investigation of sources of error associated directly with the sampling technique.

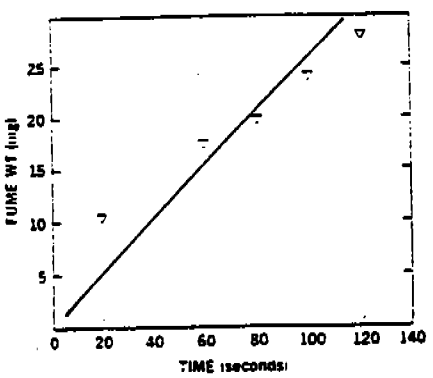

Fig. 3 — Collection linearity of a single filter as a function of time

Although there is some evidence of a variation in fume formation for different plates, the effect can be minimized, as far as relative measurements are concerned, by collecting a given series of weld data on the same plate. In absolute terms, the variation is a source of error on the order of a percent or two. Such an error is insignificant when compared to other sources yet to be discussed.

Work travel speed can also be omitted in the specification of FFRs. Increasing the travel speed by a factor of two produces a 5% decrease in the formation rate. Small variations in work travel speed from nominal values have, therefore, no significant effect. The observed variation is also not great enough to warrant specifying travel speed when stating the fume formation rates.

Depending on the shield gas, voltage and current are by far the most important factors among the welding parameters. For argon-based shielding gas, a 1 to 5% variation in voltage for a fixed current can produce changes in the FFR of as much as 20%. By way of contrast, the sensitivity of the FFR to changes in the voltage and current is far less for CO_2 shielding gases. In terms of reproducibility of the results, one must exercise great care in maintaining the voltage and current settings when welding with the argon-based shielding gases. In this regard, the ability to measure the arc length is exceedingly useful.

From the above information, it was expected that the FFRs would be reproducible to within 10%, yet statistical fluctuations of as high as 40% were observed. The large standard deviations that resulted tended to reduce the statistically meaningful information which could be extracted from the data. As a result, the sampling method was explored as the source of the problem. The sensitivity of the fume generation rate to the fume collection rate was examined. Different fume collection rates produced statistically consistent FFRs as long as isokinetic sampling conditions were maintained. However, an investigation of the sensitivity of the FFR to the sampling period revealed that the problem resided in variations in the stopping power of the filters. This data is presented in Figs. 2 and 3. In Fig. 2, ten welds were made at a constant sampling rate. All conditions were held constant except for the sampling period which was increased by 10 seconds for each successive weld. In principle, all the points should be on a straight line passing through the origin. The slope of this line is proportional to the FFR. Instead of a straight line, a wide scatter was observed as Fig. 2 demonstrates.

In addition to the data, there are four lines drawn in Fig. 2. The outer lines represent the worst case slopes for all the data points. There is a factor of six difference between them. The inner lines are the worst case slopes for the data where the sampling period was greater than or equal to one minute. The longer sampling period tends to reduce the variations in the filters. In this case, the slopes are within 40% of one another. It should be remembered that these are worst case slopes. The accuracy can be further improved by making a least squares fit and limiting the sampling periods to one minute or greater. This results in an overall statistical accuracy of approximately 20% for the absolute measurements of the FFRs cited in this report.

The behavior of individual pieces of filter paper was also examined as a function of time. The same piece of filter paper was successively exposed for constant time increments and weighed after each increment. These results are plotted in Fig. 3. In this case, the points lie on a straight line, as expected, although there appears to be a nonlinearity during the initial few seconds of sampling. This does not present a problem since the information can be drawn from the linear portion of the curve. Equally important is that over typical sampling periods of one or two minutes, no saturation of the filter was observed. In fact, no saturation was observed even with sampling periods as long as four minutes for many welding processes.

To summarize, therefore, absolute measurements of the FFRs are subject to large variations. Voltage and current must be precisely determined and maintained. Plate variations and work travel speed, although factors, do not result in significant variations. Differences from filter to filter account for the largest and least controllable variation. As a result, FFRs can be conveniently determined within no more than 20%. Greater accuracies are possible but are not required for the purpose of the comparisons made in this article.

Table 1 — Fume Sampling in SMA Welding

Class	Electrode Brand	Diam	Current	Voltage	Polarity	Fume formation rate g/min	mg/g
6010	A	5/32	110	29	RP	.32	19
6010	A	5/32	170	31	RP	.66	24
6012	B	5/32	108	20	SP	.12	7
6012	B	5/32	190	21	SP	.25	9
7018	B	5/32	160	22	RP	.28	8
7018	B	5/32	220	26	RP	.65	18
7024	C	5/32	180	32	RP	.29	8
7024	C	5/32	230	36	RP	.47	8
7024	C	5/32	180	30	SP	.29	7
7024	C	5/32	250	37	SP	.50	9
7024	D	3/16	230	36	RP	.54	9
7024	D	3/16	250	36	RP	.58	9
7024	C	3/16	250	34	RP	.39	7
7024	C	3/16	220	32	RP	.31	7
7024	D	3/16	230	30	SP	.50	9
7024	D	3/16	250	32	SP	.56	9
7024	C	3/16	230	32	SP	.48	9
7024	C	3/16	250	34	SP	.68	13
308-16	E	5/32	160	23	RP	.25	10
308-16	E	5/32	210	28	RP	.51	16

Particulate Data by Process

General

Firm limits exist for both the time weighted and excursion levels of solid materials dispersed in air. These limits are rather arbitrary, although some toxicological data exist to support them. They are deficient in that they fail to recognize that variations in crystallographic structure, particle size, and chemical activity are important in influencing the interaction of such materials with the human system. We have studied fume generation in several arc welding processes: shielded metal arc (SMA), flux cored arc (FCA), gas metal arc (GMA), and gas tungsten arc (GTA) welding. Fume generation is measured in two ways: g of fume/min of arc time and mg of fume/g of metal deposited. These formalisms (g/min and mg/g) express the relative "cleanliness" of a process on real time and real completion rate bases.

FFR measurements were made on 200 × 250 mm fiberglass filters using the techniques described in the previous section. Samples for compositional analysis were made on triacetate filters and analyzed using atomic absorption spectrophotometry and x-ray fluorescence techniques. A limited amount of size distribution data has been taken.

SMA Welding

Only electrodes for the welding of ferrous materials were studied. These electrodes include those of the cellulosic type, rutile type, rutile-iron powder type, and low hydrogen type. Both dcsp and dcrp were studied wherever possible. A constant current type power supply was used. Results are briefly summarized in Table 1.

The FFR data (mg/g) is plotted against current in Fig. 4 for 5/32 in. electrodes. Data reduced from Refs. 2, 3, and 4 are also included. Note that the data fall into three bands. The lowest FFRs are associated with rutile and rutile-iron powder type electrodes. Higher rates are found for low hydrogen type electrodes, probably due to the presence of CaF_2 in the flux. Cellulosic electrodes have the highest rates.

Variations in rates accompanying polarity changes are best understood by variations in arc voltages due to the polarity change.

No chemical analyses were performed on SMA welding fume. It is expected that the principal difference between fume from rutile, rutile-iron powder electrodes, and from low hydrogen electrodes will be the presence of CaF_2.

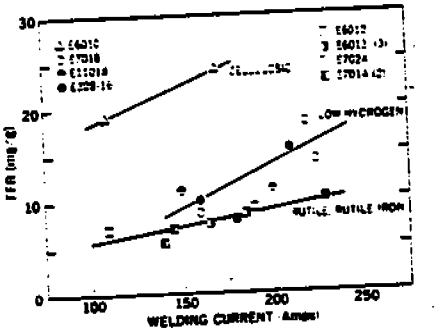

Fig. 4 — Comparison of FFRs for several SMA electrodes

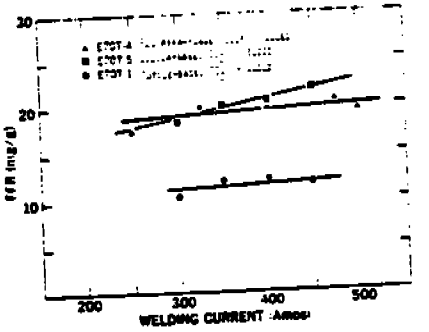

Fig. 5 — Comparison of FFRs in FCA welding for three electrodes

FCA Welding

Three types of flux cored electrodes were studied: CO_2 shielded,

Table 2 — Fume Sampling in FCA Welding

Electrode Designation	Brand	Current	Voltage	Shielding gas	Fume formation rate g/min	Fume formation rate mg/g
E70T-1 Rutile-base	D	300	28	CO_2	.75	11
		350	30		.96	12
		400	31		1.10	12
		450	32		1.20	11
E70T-5 Silica-base	E	300	28	CO_2	1.40	18
		350	29		1.90	20
		400	30		2.10	21
		450	31		2.50	22
E70T-4 Fluorspar-base	B	250	29	None	1.08	18
		325	30		1.62	20
		400	31		2.00	20
		475	32		2.50	20

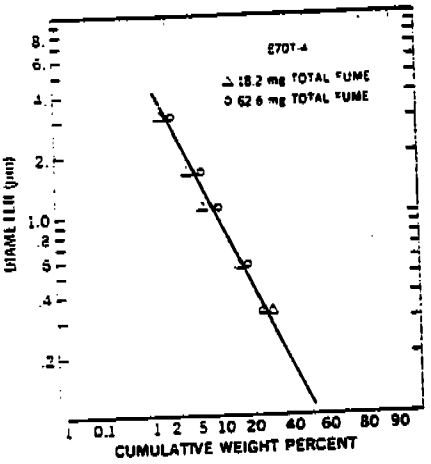

Fig. 6 — Particle size distribution by weight percent in FCA welding

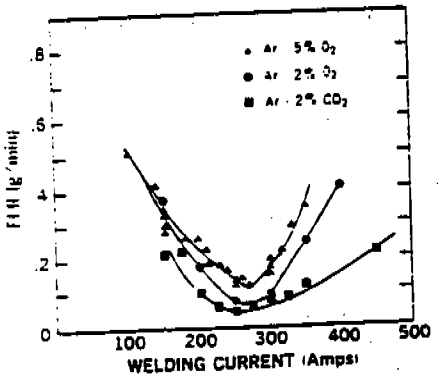

Fig. 7 — Comparison of FFRs in GMA welding using argon-based shield gases

silica-base (E70T-5); CO_2 shielded, rutile-base (E70T-1); selfshielded, fluorspar-base (E70T-4). A constant potential type power supply was used. The results of the fume generation studies are shown in Table 2.

Figure 5 shows a combined plot of /g versus current for the data. ..ere is an appreciable difference in FFR between selfshielded, fluorspar-base and CO_2 shielded, rutile-base electrodes. A similar difference is noted between CO_2 shielded, silica-base and CO_2 shielded, rutile-base electrodes. These differences are primarily due to variations in arc stability and CaF_2 content.

Table 3 shows the comparative and absolute variations in fume composition for the three types of electrodes. Note that the rather large variation in fume composition results from differences in the flux compositions.

Variations in welding parameters did not seem to have a significant effect on FFR. Voltage increases did not produce FFR increases in any way comparable with those found in SMA welding.

Particle size distribution data were taken using an inertial separation system. The results of two of the studies with the selfshielded, fluorspar-base electrode are shown in Fig. 6. The plot shows the cumulative weight percent of fume due to particles larger than any diameter. The weight distribution is log-normal. The mean particle size by weight calculated from this data is 0.12μm.

GMA Welding

Particulate data were gathered in GMA welding with a variety of wire compositions, wire sizes, and shielding gases over a broad range of welding conditions. General considerations on reproducibility and technique were discussed in previous sections of this article. This section covers additional work on ferrous materials and aluminum alloys.

Ferrous Materials

Effect of Shielding Gas on FFR. Treating first the effect of shielding gas, reference is made to Figs. 7 and 8. Figure 7 shows the FFR plotted against current for argon-base shielding gases. The wire diameter was 0.045 in. and the welding voltage was 28 V. Note the presence of a well defined minimum in the 250-300 A range for each of the shielding gases. Figure 8 plots FFR versus current for CO_2 and Ar-25% CO_2. For these gases FFR is a monotonic function of current. Note that significant, reproducible departures from the Ar-25% CO_2 curve occur at 300 and 400 A.

A comparison of these figures reveals that considerably more fume is produced when welding with CO_2 shielding compared with argon-based shielding. The explanation of this effect involves consideration of the oxidizing nature of the shield gas and of the mode of metal transfer.

The dependence of the FFR on the oxidation potential of the shield gas was examined by measuring the FFR as a function of the oxygen content of an argon-based shielding gas. These results are shown in Fig. 9 for O_2 additions of up to 40%. Note that the FFR is approximately equal to $(\%O_2)^{3/4}$. Since oxygen is present as atomic oxygen in the arc to a certain extent, it is possible that the dependence would be greater than $(\%O_2)^{1/2}$. Thus the exponent ¾ is reasonable.

Effect of Welding Parameters and Wire Size on FFR. The existence of the minimum in FFR noted above for argon-based shielding gases was explored further as a function of welding parameters. Figure 10 shows constant current plots as a function of arc voltage for FFR (g/min). In all cases, arc length increased for increasing arc voltage. Note that the minimum FFR occurs at 28 V, 250 A. If mg/g is used as a criterion instead, a similar observation is made. Fig. 11. The minimum correlates with the transition from globular to spray transfer. This minumum is thought to result from the establishment of a stable spray arc at a minimum voltage.

Similar plots for CO_2 shielding gas are shown in Figs. 12 and 13. Note the absence of any minima. This observation reinforces the hypothesis that the transfer mode affects the FFR.

Figure 14 shows the effect of wire diameter on FFR in Ar-5%O_2.

Fume Composition and Particle Size Distributions. Fume composition was measured for a number of welding conditions. Data may be found in Table 4. For the most part, as measured by weight percent, the composition of the fume is constant. The most significant exception to this is that the fume silicon contents generated in argon shielding gas are significantly less than those produced with oxygen bearing argon-based gases and substantially less than CO_2.

Particle size analysis of the fume produced using argon-based shielding gases and CO_2 shielding gases was attempted. However, when argon-based shielding was used, no fume could be collected on the upper

stages of the sorter. Electron micrographs revealed fume particle sizes on the order of 0.005 to 0.1 microns. These particle sizes are much smaller for any other welding process explains the null result with the er. A visual comparison of particle is presented in Fig. 15.

The particle size distribution measurements for CO_2 shielding gas were made at 300 A, 34 V. The results are plotted in Fig. 16. An extrapolated mean particle diameter of 0.03 micron, considerably smaller than for FCA welding, is determined from this data.

Aluminum Alloys

FFRs and fume compositions were determined for 1100 and 5356 alloys welded in argon. Typical FFRs (g/min) and fume compositions are given in Table 5.

It is interesting to note the decrease in FFR with increasing current. This observation is similar to that observed in GMA spray arc welding of steel over a certain range of current and voltage. A precise understanding of this effect is lacking at this time.

GTA Welding

Fume formation in GTA welding of steel using 3 mm and 5 mm thoriated tungsten electrodes with argon shielding gas was studied. The FFRs for all currents between 50 and 450 A were essentially zero.

Discussion of Results and Probable Mechanisms

In addition to supplying comparative data among different arc welding processes, it was believed that the FFRs and the composition of the welding fume could help to identify the mechanism of fume formation.

Consider first free elemental vaporization as a source of fume. The partial pressures of Mn, Si, and Fe above molten steel with the composition of the E70S-2 electrode are plotted as a function of temperature in Fig. 17. Two things are apparent. Free vaporization can account for the increase in fume with arc temperature, but based on this mechanism alone there should be but negligible silicon in the fume compared with Mn and Fe. Since this is not the case, other mechanisms must contribute.

The notable difference in fume composition between weldments made in argon-based gases and CO_2 is the silicon content of the fume. The same difference, although somewhat smaller in magnitude, exists between fume produced with Ar-2%O_2 and Ar-5%O_2. This suggests that oxidation may be important in producing fume containing silicon. The supporting data, drawn from Table 4, are indicated below:

Current, A	% Si for shielding gases of: Ar	Ar-2% O_2	Ar-5% O_2	Ar-25% CO_2	CO_2
250	2	5	14	—	25
300	1	7	14	17	27
360	4	10	14	—	—

Table 3 — Fume Composition in FCA Welding [a]

	E70T-1 %	E70T-4 %	E70T-5 %
Fe	28	13	23
Mn	5	2	4
	25	4	20
	—	13	8
	2	—	—
	2	—	—
Mg	3	9	—
Al	—	9	—
F	7	13	7

	E70T-1 mg	E70T-4 mg	E70T-5 mg
	2.1	1.8	3.3
Mn	.4	.3	.6
	1.8	.5	2.9
	—	1.8	1.1
	.2	—	—
Mg	.2	1.2	—
Al	—	1.2	—
F	.5	1.8	1.0

[a] E70T-1, rutile base flux, CO_2 gas shielding; E70T-4, fluorspar base flux, no gas shielding; E70T-5, silica base flux, CO_2 gas shielding.

Table 4 — Fume Formation Composition in GMA Welding of Ferrous Materials

Shield gas	Current	Voltage	FFR mg/min	Mn %	Si %	Fe %	O %	Mn mg/min	Si mg/min	Fe mg/min
Argon	250	29	35	4	2	63	31	1	1	22
	300	31	25	4	1	46	49	1	0	12
	350	35	98	5	4	52	39	5	4	51
Ar-2%O_2	150	28	257	6	3	52	39	15	8	134
	200	28	147	8	7	51	34	12	10	75
	250	28	37	8	5	70	16	3	2	26
	300	29	56	9	7	63	22	5	4	35
	350	31	115	9	10	50	31	10	11	58
	400	34	162	11	10	53	26	18	16	86
Ar-5% O_2	100	28	557	5	6	49	40	29	33	273
	150	28	299	5	7	50	37	16	21	150
	200	28	257	6	9	50	35	16	22	129
	250	28	140	7	14	43	36	10	20	60
	300	28	162	6	14	47	33	10	23	76
	300	28	169	5	14	41	40	9	23	70
	80	20	110	9	11	56	24	10	12	62
	120	20	140	9	14	51	26	13	20	71
	200	20	162	9	18	52	21	15	29	84
Ar-25% CO_2	100	23	120	9	17	63	12	11	20	75
	150	27	210	6	17	50	27	13	35	105
	300	35	367	8	17	52	23	29	62	191
CO_2	130	27	198	7	30	43	20	13	59	86
	150	30	264	5	24	45	25	14	63	120
	180	30	321	7	26	47	21	22	83	150
	200	30	279	7	26	45	22	19	73	126
	250	30	449	7	25	48	20	31	112	216
	300	30	455	8	27	47	18	36	125	214
	140	22	198	7	32	43	18	14	63	85

Much work has been done studying the properties of SiO. Silicon monoxide is a gas at all temperatures of interest, 1500-3000 K. It is often formed when insufficient oxygen is available to form continuous SiO_2 layers over silicon-bearing liquids. It has a high vapor pressure. The reaction of interest is:

$$Si + \tfrac{1}{2} O_2 \rightarrow SiO, \text{ or} \quad (1)$$
$$Si + CO_2 \rightarrow CO + SiO \quad (2)$$

The standard free energy of each of these reactions may be calculated from thermodynamic data (Refs. 5, 6). Consider Equation (1) for the E70S-2 electrode composition, $a_{Si} = 3.35 \times 10^{-5}$; the partial pressure of SiO (P_{SiO}) as a function of temperature is:

Temp. (K)	Partial pressure P_{SiO} (atm) for P_{O_2} (atm) = .01	.02	.05
2000	.097	.137	.217
2500	.023	.033	.051
3000	.009	.013	.020

Obviously, since the reaction is controlled by $(P_{O_2})^{1/2}$, the ratio of P_{SiO} at any temperature in equilibrium with Ar-5%O_2 to that in equilibrium with Ar-2%O_2 is $(5/2)^{1/2}$ or 1.58. If equilibrium thermodynamics can tell us anything about the relative fume formation, then we should measure this increase in silicon in our fume samples. The actual ratios, at each set of welding currents, for silicon emission from Table 4 are:

Current, (A)	Si (5% O_2) / Si (2% O_2)
150	2.6
200	2.2
250	10.0
300	5.7

Interpretation of these results is uncertain because of possible variations in arc behavior; however, it is apparent that the generation of silicon-bearing fume is dependent on oxidation potential. If we now perform the calculations for Equation (2) and assume that the stoichiometry of the reaction as written applies, we find:

Temp. (K)	P_{SiO} (atm)
2000	.290
2500	.508
3000	.672

Thus, we would expect significant increases in the rate of silicon emission, when CO_2 is present in the shielding gas, as great as an order of magnitude. It is not reasonable to compare data taken in Ar-2%O_2, Ar-5%O_2, and CO_2 except under conditions of globular transfer. The only data points are at 150 A, and caution must be used because the arc lengths vary significantly. Data from Table 4 show:

$Si(CO_2)/Si(5\%O_2)/Si(2\%O_2)$
$= 7.9/2.6/1.0$

Further comparisons are not justified. If we solve Equation (2) with $P_{CO_2} = .25$, for Ar-25%CO_2 we obtain:

Temp. (K)	P_{SiO} (atm)
2000	.123
2500	.185
3000	.216

Silicon emission should now be roughly the same as it is for Ar-2%O_2 and Ar-5%O_2 in the temperature range 2000-2500 K. The data of Table 4 agree with these calculations.

What then of vaporization of FeO and MnO as contributors to fume generation? The calculations for FeO are tabulated below, for three partial pressures of oxygen:

Temp. (K)	P_{FeO} (atm) for P_{O_2} (atm) = .01	.02	.05
2000	.003	.005	.007
2500	.039	.055	.087
3000	.204	.288	.456

The calculations in CO_2 yield:

Temp. K	P_{FeO} (atm) for P_{CO_2} (atm) = .25	1.0
2000	.003	.007
2500	.054	.115
3000	.198	.567

Changing from Ar-5%O_2 to CO_2 does not alter the FeO contribution significantly. The same is true for changing from Ar-2%O_2 to Ar-25%CO_2. The data agree with these calculations. For the temperature and ranges of Mn activity of interest, no significant amounts of MnO form.

Based on the above, it can be understood why fume generation is significantly less in the GMA welding process when argon-based shielding gases are employed than when CO_2 is used, and why there is a suppression of the silicon content of the fume. Both of these facts support the hypothesis that fume generation is the sum of elemental vaporization and oxide vaporization. It is felt that the Mn component comes strictly from elemental vaporization, the Si component from SiO formation, and the Fe component from elemental plus FeO vaporization. FFRs with argon-based shielding gas are lower because there is no enhanced vaporization due to oxide species as the data drawn from Table 4 indicate:

Current, A	FFR (g/min) Ar	2% O_2	5% O_2	25% CO_2	CO_2
250	35	37	140	—	449
300	25	56	162	367	455
350	98	115	—	—	—

The mechanism of fume formation appears to be, therefore, one of ele-

Table 5 — Fume Formation Rate and Composition in GMA Welding of Aluminum Alloys

Alloy	Diam	Current	Voltage	FFR (g/min)	Fume composition % Al	% Mg
5356	.045	150	24	1.10	45	5
5356	.045	200	25	.95	46	6
5356	.045	250	27	.85	47	8
5356	.045	300	28	.70	40	11
1100	.035	130	23	.70	50	0
1100	.035	210	26	.60	50	0

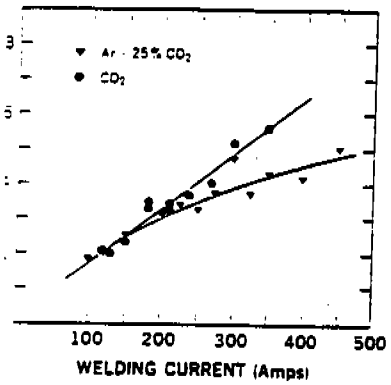

Comparison of FFRs in GMA ...ing using shield gases containing ...e than 25% CO_2

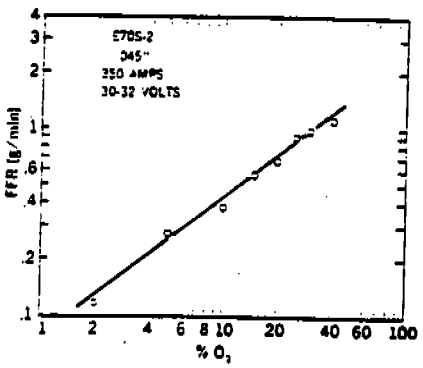

Fig. 9 — The effect of oxidizing potential on the FFR in GMA welding

mental vaporization, condensation, and oxidation enhanced vaporization.

Additional support for the vaporization-condensation-oxidation mechanism (V-C-O) is also found in the data presented in Table 5 covering GMA welding of aluminum alloys. Because of inert shielding, the mechanism for fume generation is simply vaporization and condensation of elemental material. Aluminum 5356 generates more fume because of the additional contribution of Mg. Note that the Mg content of the 5356 fume (Mg/Al = 1/8) is enriched over that of the wire (Mg/Al = 1/16). This results from the fact that Mg has a considerably higher vapor pressure in the range of 2000-3000 K and its activity coefficient in liquid aluminum is 0.5. In making a comparison of the above data, note that finer wires produce less fume at comparable currents and arc lengths. The above discussion applies equally well to fume generation in FCA and SMA welding. In these processes, the fume results from the V-C-O of elemental and lower oxide species, and the V-C of oxide and fluoride flux species. As might be expected, the composition of the fume is strongly dependent on flux composition since significant quantities of low melting point flux components are contained in the fume.

The V-C-O mechanism advanced to this point is essentially a simple one having to do with the vapor pressures and latent heats of vaporization of the constituents present in the core of the consumables and with the oxidizing potential of the shielding gas if one is used. To first order, these factors determine the amount of a particular constituent appearing in the fume. Obviously, rate controlling steps involving diffusion of the various reactants and products will affect the FFR and composition of the fume as well. A more complete model requires consideration of these rate controlling factors and the dynamic nature of the metal transfer process including such factors as residence time of the molten droplet at a particular temperature, degree of surface exposed for participation in the vaporization process, and the efficiency of energy absorption by the surface. These contributions will be considered in turn.

For instance, as observed previously, the higher FFR for CO_2 compared with argon-based shield gases is believed to be caused by the greater contribution of oxide species resulting from the increased oxidizing potential of the CO_2 shielding gas. Additionally, the inability to achieve rapid drop detachment when using CO_2 may further augment the oxide enhancement. With CO_2, the molten drop of metal spends a significant fraction of the total transfer time attached to and wandering about the wire tip. This instability can produce turbulent effects resulting in contamination which, coupled with the long detachment times, can further enhance the vaporization due to oxide species over and above the natural oxidizing potential of the shield gas. The rapid drop detachment obtained in the spray mode using argon-based shield gases does not permit this condition to occur. This fact and the lower oxidizing potential of the argon-based shield gases are sufficient to account for the differences in the mean FFRs.

The problem of instabilities and turbulent effects in FCA and SMA similar to those which exist with CO_2 in GMA is compounded by the presence of extremely volatile flux components. Hence, the FFRs for these processes are substantially higher than for GMA.

In an effort to gain more precise information about how these dynamic effects affect the V-C-O process, it was felt necessary to determine where the vaporization is occurring. Two experiments were performed. The first was to examine fume formation using the GTA process. As stated earlier, no measurable amounts of fume were obtained for all currents between 50 and 450 A using argon shielding. The initial implication is that the molten metal in the weld puddle does not substantially contribute to the fume. The weld puddle is cool relative to the arc. While vaporization is occurring, the partial pressures and hence the contribution to the total fume level is substantially reduced. Adding oxygen to the shielding gas did produce small amounts of fume, supporting the hypothesis of enhanced vaporization due to oxide species.

The second experiment involved the welding of Mg bearing Al plate using the GMA process. Two wire types were employed, type 5356 containing Mg and type 1100 containing no Mg. Referring back to Table 5, Mg was found in the fume when the 5356 wires were used, but no Mg was found when the 1100 wires were used even though Mg was present in the plate in both cases. The conclusion to be drawn, therefore, is that the vaporization of elemental and oxide species is occuring at the wire tip and in the welding arc, but not in the weld puddle to any comparable degree. This is totally consistent with known temperature distributions of the arc.

A feeling for just how the fume evolution is affected by the welding conditions and shielding gas can now be gained by a more critical examination of the behavior of the fume data in CO_2 and argon-based shielding gases exhibited in Figs. 10 and 12.

The CO_2 results are presented in Fig. 12. Two features are apparent. For a given voltage, there is a monotonic increase of fume with current;

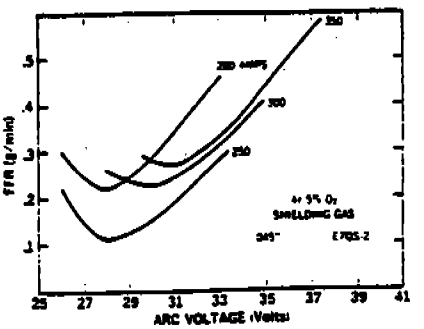

Fig. 10 — The effect of voltage and current on the FFR in GMA welding with argon-5% O_2 shielding gas

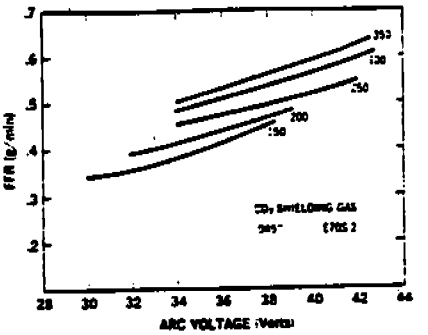

Fig. 12 — The effect of voltage and current on the FFR in GMA welding with CO_2 shielding gas

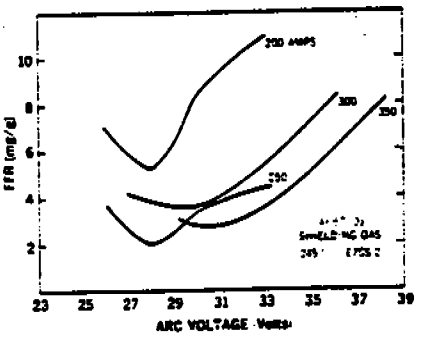

Fig. 11 — Data of Fig. 10 replotted in mg/g

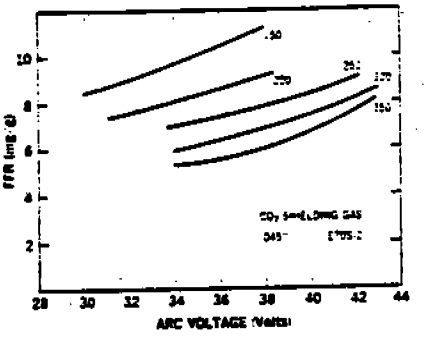

Fig. 13 — Data of Fig. 12 replotted in mg/g